Effect of Turbine Upstream Geometry on Pulsating Flow and Turbocharged Si-Engine Performance

THE EFFECT OF TURBINE UPSTREAM GEOMETRY ON PULSATING FLOW AND TURBOCHARGED SI-ENGINE PERFORMANCE

Jeyoung Kim[1,2)], Meng Soon Chiong[2)] and Srithar Rajoo[2)]

[1)] University of Vaasa, School of Technology and Innovations, Wolffintie 34, FI-65200 Vaasa, Finland
[2)] UTM-LoCARtic, IVeSE, Universiti Teknologi Malaysia, Johor 81310, Malaysia

1. INTRODUCTION

Turbocharging system has been a common technology in the automotive industry as it increases specific power (kW/L) which enables engine downsizing. With a smaller engine, the higher output can be achieved by delivering pressurized air into the combustion chamber while recovering energy from the exhaust. The smaller engine with fewer cylinders has less friction, heat transfer, and mass so that it has better fuel consumption and fewer emissions. In addition, turbocharging has been known as the most cost-effective way to reduce tailpipe CO2 and improve fuel economy (Alshammari et al., 2019; Bassett et al., 2017; Turner et al., 2014). For these reasons, most global automotive OEMs have increased turbocharged lineup in their portfolio to comply with continually stringent regulations over the last two decades.

In the EU, nearly every two out of three vehicles are turbocharged which indicates 67 % of market penetration (More, 2020). In the US, 34 % of the light-duty vehicles for the model year 2019 adopted turbocharging system (US EPA, 2020). Even though the steady growth of implementing the turbocharging system in internal combustion engines (ICEs) has been observed, the global market is currently moving forward to electrification such as electric vehicles (EVs) or fuel cell vehicles (FCVs). With growing momentum on phasing out ICEs globally starting from as early as 2025 and 2035 in Norway and the EU respectively, its shift would be accelerated rapidly.

However, there are several factors to impede the expansion of EVs such as their high cost, charging speed, driving range, battery safety, battery recycling issue, lack of charging infrastructure, and well-to-wheel CO2 emissions (Lou and Zhu, 2020). In addition, gasoline and diesel fuel have 80 times higher energy density (J/kg) compared to the highly efficient lithium-ion battery at the current stage (Brace, 2020). In the case of FCV, it has zero emissions and quick fueling & long driving range comparable to ICEs, but the downsides are high cost, lack of charging stations, and immaturity of the technology (Lou and Zhu, 2020).

Both vehicle systems have not been fully matured yet and still need to be improved further. It would take some time to invent breakthrough technologies and expand its infrastructure. Therefore, in the short-to-medium term, ICEs would survive and remain as the main power source in the transportation sector but in the forms of hybridization or advanced ICE concepts (Reitz et al., 2020). In this case, advanced charging systems will play an important role.

For the hybrid powertrain, an electrically assisted boosting system not only helps to improve engine thermal efficiency, low-speed torque, and transient response but also regenerates energy (Alshammari et al., 2019; Shahed, 2006; Terdich et al., 2014; Xue and Rutledge, 2017). In addition, the advanced boosting systems help to implement advanced strategies such as Miller cycle or variable compression ratio (VCR) for further improvement of efficiency (Al-Hasan et al., 2015; Christmann et al., 2020). Hence, it is expected that more turbocharged ICEs would appear on the market which have better fuel economy and lower emissions.

The turbocharging system basically consists of two units which are a turbine and a compressor. Each component is connected by a single shaft. In general, one set is commonly utilized as a single-stage charging system. However, 2-stage boosting system can be utilized for high-performance & luxury or heavy-duty vehicles. The turbine recovers the energy from the exhaust flow and generates the power to be utilized by the compressor. In the automotive application, a pulsating charging system has been widely used where the turbine is driven by pulsating exhaust flow which carries a large amount of pressure energy and a small portion of kinetic energy by combustion (Watson and Janota, 1982). Thus, how well this large amount of energy is transferred to the turbine and its utilization are keys to efficient energy recovery.

In order to take advantage of pulsating energy more effectively, various research has been carried out. One of them is a multi-entry turbine such as a double-entry or twin-entry system. Both systems have two inlet scrolls which enable isolating exhaust pulses. Thus, the pulse overlaps or interaction between individual exhaust pulses from each cylinder can be avoided. As a result, the loss of exhaust pulse energy is reduced, and more energy can be transferred to the turbine which

is able to extract more power. It showed that the twin-entry turbine increases torque and power up to 14 % in low engine speed regions from 1000 to 3000 RPM (Kusztelan et al., 2012). It is observed that the twin-entry turbine has relatively low fuel consumption (-2.7 %) compared to the single-entry turbine under WLTC drive cycle test (Chiong et al., 2019).

Another evolution is active control turbine (ACT) which is invented by Imperial college turbo group. ACT has variable nozzle vanes like VGT. However, the movable nozzles are controlled by instantaneous exhaust pressure pulses to capture unsteady flow more effectively (Feneley et al., 2017). As a result, 7 % higher energy recovery, 5 % higher engine brake power, and 0.5 % better thermal efficiency are reported (Cao et al., 2015; Pesiridis, 2012; Rajoo et al., 2013). Even though it is not commercialized, its benefit of utilizing pulsating energy is remarkable.

Most previous studies have focused on refining turbine design or turbocharger itself. Recently, several studies have examined the effect of exhaust geometry on turbocharger and engine performance to exploit unsteady pulsating flow energy efficiently. Lim et al. (2018) carried out a numerical study using detached eddy simulation (DES) to investigate the influence of exhaust manifold on pulse flow turbine performance. It revealed that its impact on heat transfer and internal irreversibilities in the scroll is significant but not for the prediction of turbine power. However, this study investigated the exhaust manifold from the perspective of turbine performance but engine performance is not considered. Anton et al. (2017) examined three different radial turbine designs to achieve high turbocharger efficiency considering unsteadiness and exhaust manifold volume using 1D engine simulation. The efficiency potential of each turbine and limitations of turbine types and turbine design are mainly discussed.

Kesgin (2015) carried out an extensive study on the effect of the exhaust geometry (length, diameter and junction of exhaust pipe) on the engine performance of the stationary natural gas engines including V12, V16, V20 engines with constant pressure turbocharging system using 1D and 3D simulation. It revealed that the diameter of exhaust manifold should be equal to at least the bore of the cylinder for ideal operation of the constant pressure charging system. Kellermayr et al. (2019) studied the influence of the number of cylinders on the pumping losses using simulation and experiments. They found that the exhaust volume has a strong effect on pumping losses. Liu et al. (2021) examined the effect of exhaust system structure (diameter of exhaust pipe and exhaust manifold) on the gas exchange performance and exhaust energy recovery using a 1D-3D coupling simulation. It is noted that the decrease in exhaust pipe diameter and exhaust manifold outlet diameter increases the exhaust energy, exhaust resistance, and pumping losses while scavenging performance decreases.

These studies recognized the importance of the exhaust or turbine upstream geometry on turbocharger and engine performance. Nevertheless, the engine performance is mainly discussed and analyzed. Even though the turbocharger performance is discussed partially, its analysis is mainly based on time-averaged or cycle-averaged data. However, the cycle-based analysis considering pulsating effect is important since the pulsating turbocharging system is driven by pulsating exhaust flow. Indeed, the pulsating exhaust flow carried the energy to the turbine. In addition, its shape and energy transmission could be influenced by the configuration of turbine upstream geometry structure. Also, the cyclic fluctuation has significant effects on the exhaust energy and its utilization (Mahabadipour et al., 2018).

In fact, the importance of the turbine upstream geometry was realized in the experimental campaign. When the authors have performed on-engine testing with several different turbine designs, it was found that the large collector volume right before the turbine has a huge impact on the pulsating pressure profile and turbine & engine performance. Therefore, in the current study, the effect of turbine upstream geometry structure on turbocharger and engine performance is investigated and analyzed while considering pulsating effect by 1D engine simulation which reduces experimental time and cost but provides reliable results and insight to understand complex results.

2. 1D ENGINE SIMULATION

2.1. Engine Model and Validation

1D engine model was generated based on a naturally aspirated (NA) inline 3-cylinder gasoline engine using AVL-BOOST. The details of the engine are presented in Table 1. Two-zone combustion model and single Wiebe function were utilized as it represents major combustion characteristics of SI engines such as initial ignition delay, rapid combustion growth, gradual decay and burn rate, reasonably (Ferguson and Kirkpatrick, 2001). For in-cylinder heat loss model, Woschni correlation was used. The heat transfer on intake and exhaust line was adjusted using scaling factors to match measured volumetric efficiency and exhaust temperature within reasonable scaling ranges.

The NA engine model is tuned and validated with experimental data. Since the NA engine model will be converted into a turbocharged (TC) model, pressure and temperature of the exhaust are key factors to influence the performance of the pulsating turbocharger. These are presented in Figure 1. Intake pressure, exhaust pressure, and exhaust temperature indicated less than 3 % error. In addition, high-frequency pressure is measured at the intake and exhaust line and used to validate airpath system and gas exchange process in the model as shown in Figure 2. It shows a rather good match over the pressure profiles with minor deviations. The general engine performance parameters including air and fuel flow rate showed good agreement within 3 ~ 10 % range (Kim, 2019). From this, it was identified that steady-state engine characteristics and dynamic flow conditions are well represented in the model.

Table 1. Engine specification.

Engine parameter	Value
Displacement	989 cc
Bore	72 mm
Stroke	81 mm
Compression ratio	10:1
No. of cylinders	3
Valves per cylinder	4 (2-intake, 2-exhaust)
Fuel injection type	Port fuel injection (PFI)
Maximum power	43 kW @ 6000 RPM
Maximum torque	88 Nm @ 3600 RPM

Table 2. Turbocharger specification.

T/C parameter	Value
Compressor wheel diameter	32 mm
Compressor trim	50
Compressor A/R	0.32
Turbine wheel diameter	30 mm
Turbine trim	72
Turbine A/R	0.18

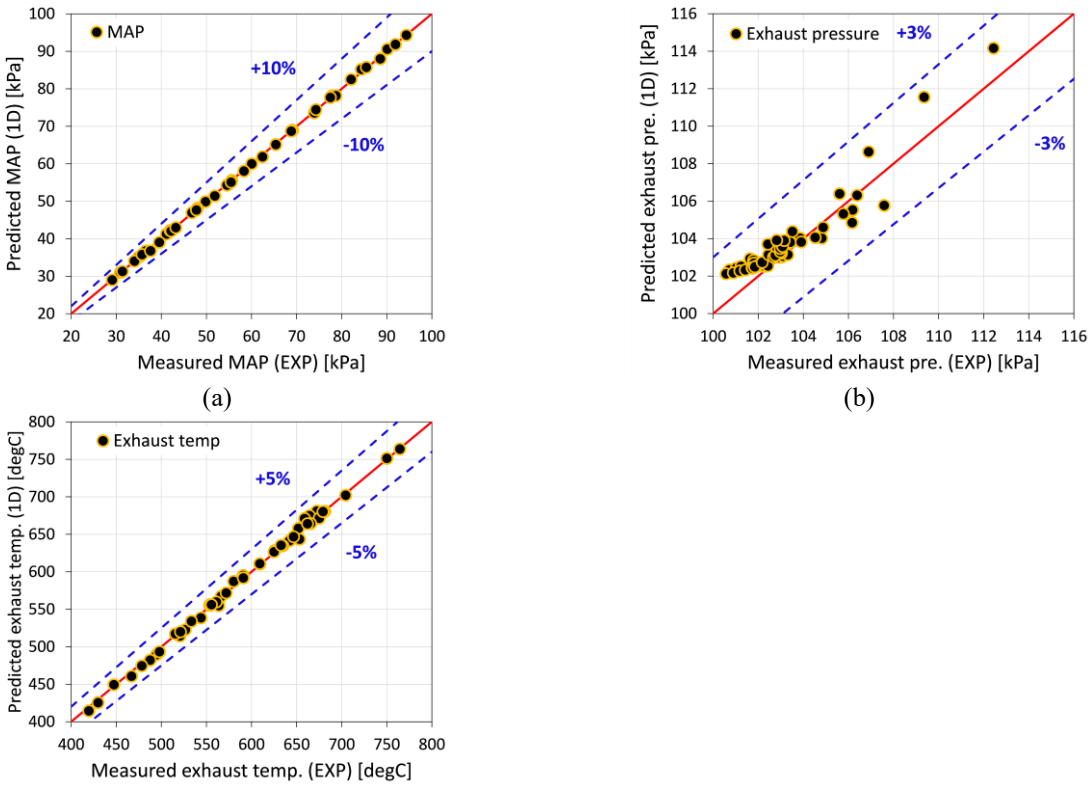

Figure 1. Validation results: (a) MAP; (b) Exhaust pressure; (c) Exhaust temperature.

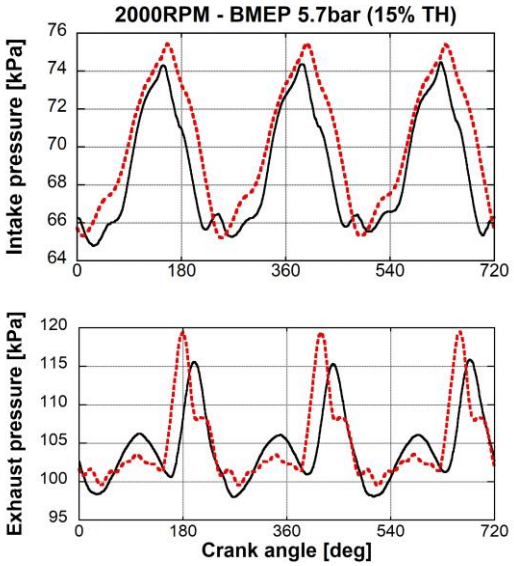

Figure 2. Validation results of instantaneous intake and exhaust pressure at 2000 RPM and BMEP 5.7 bar

In-cylinder pressure is not measured in this work, as the main objective of this study is to examine how exhaust geometry interacts with the turbocharger and engine instead of the combustion analysis. Hence, high-frequency pressure data was utilized to increase the reliability of the model. Considering that instantaneous intake pressure, intake temperature, and air flow rate are well captured in the model, it is assumed that the model well replicated the condition at IVC. Then, the combustion model was tuned to match the torque or BMEP. After the combustion, exhaust pressure and temperature indirectly indicate how well the combustion model is tuned. Since pumping losses and gas exchange process are well agreed, the predicted in-cylinder pressure would not be that far from the real value. Also, the knocking was monitored in the simulation using the two-zone combustion model.

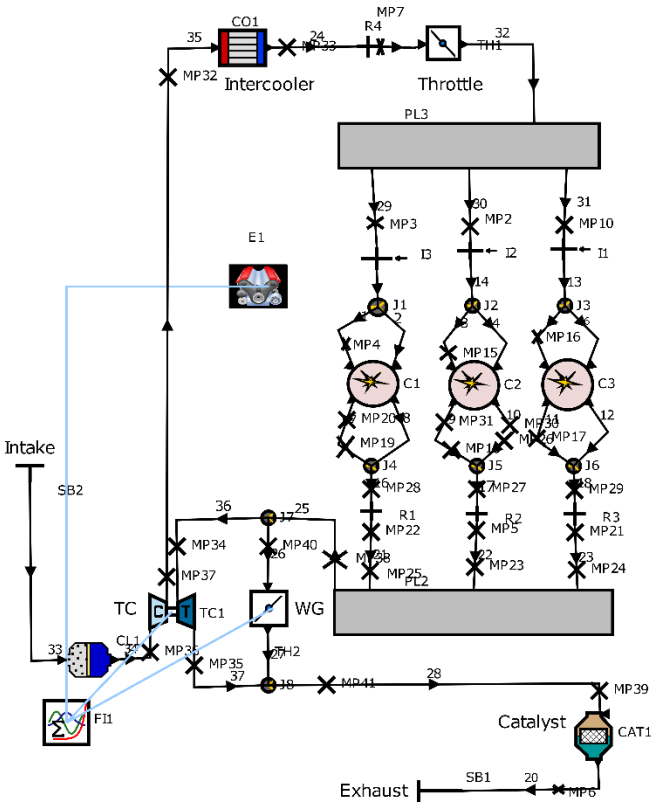

Figure 3. 1D engine model with a turbocharger.

2.2. Model Modification and Simulation Setup

From the validated NA engine model, it is converted to accommodate the turbocharger required for the current study as shown in Figure 3. Firstly, the turbocharger component is added. A turbine is added between downstream of the exhaust manifold and upstream of the catalyst. A compressor is added after the air filter which is driven by the turbine. Then, the matching between turbocharger and engine was carried out which is a crucial process. It is vital to select the correct turbocharger which could swallow the required mass flow and provide the required boost pressure by engine requirement. If a bigger turbocharger is used, it would operate at low efficiency and low-pressure ratio region. Hence, the high boost pressure is not achievable. Also, the big turbocharger will slow down transient response and would cause turbo-lag. In the case of using a smaller turbocharger, the turbocharger would perform at surge and choking regions. For this reason, the turbocharger is not able to produce high boost pressure and is suffering from an unstable operation. Using 1D simulation, Garrett GT0632SZ was selected. Its specifications are presented in Table 2. The basic compressor and turbine map are given as input and then interpolation and extrapolation are numerically carried out to extract the entire map in AVL-BOOST, internally.

The Euler equations, which are governing equations for one-dimensional pipe flow are numerically solved at each of the discretized cells. The time step is internally controlled by complying with CFL criterion which is a stability criterion defined by Courant, Friedrichs, and Lewy (AVL, 2014). To minimize simulation time, convergence control was applied. As convergence criteria, turbocharger rotational speed and its fluctuation are monitored. The tolerance of the rotational speed is set as 10 RPM /$\sqrt{k}$ which is less than 0.2 % of the minimum shaft speed on the compressor map. If the fluctuation of the rotational speed is within the tolerance over 50 consecutive cycles, the steady-state simulation is considered converged and terminated.

Once it is confirmed that the turbocharged model is working without any issues, the parametric study is conducted at the fixed operating point. Ignition timing is maintained and WG is fully closed to maximize boosting Figure 3. 1D engine model with a turbocharger. effect. Hence, its effect on the engine performance can be observed. Based on the analysis of the parametric study, further investigation has been carried out.

3. RESULTS AND DISCUSSIONS

3.1 Volume of Exhaust Manifold

To investigate how the volume of the exhaust manifold influences pulsating pressure pulses as well as engine and turbocharger, the simulation was conducted over three different manifold volumes (V/V0 = 0, 0.5, and 3, V0 = 1 L). In the case of V/V0 = 0, the exhaust line was directly merged to one junction instead of the exhaust manifold and then connected to the turbine upstream pipe. The modified exhaust line is shown in Figure 4.

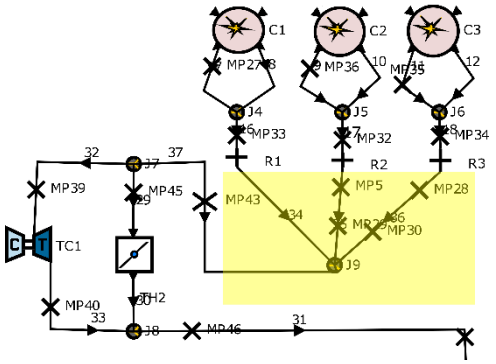

Figure 4. Modified exhaust line to reflect zero volume.

The simulation results are presented in Figure 5. Figure 5 (a) represents instantaneous pressure pulses at the turbine inlet over one cycle in solid lines. The dashed lines indicate mean exhaust pressure over the cycle. There are three peaks observed which are resulted from firing at each cylinder. It can be seen that the zero-volume (V/V0 = 0) achieved the higher peak pressure at the turbine inlet, while the large manifold (V/V0 = 3) obtained the lower peak among the three cases. The peak pressure of the zero volume is 1.6 times higher than that of the large manifold. As a result, the mean pressure is also increased at the zero-volume manifold. In addition, it is noticed that the shape of exhaust pressure pulses is extended in both upward and downward directions with the reduced volume which increased the available energy.'

A large portion of the pressure energy is released during blow-down phase where the highest peak of the pressure is observed. This sudden pressure rise accounts for generating the highest amount of turbine power as seen in Figure 5 (b). The higher peak of the instantaneous turbine power corresponds to the higher peak of the exhaust pressure since the turbine is driven by pulsating exhaust flow. Its relationship is clearly shown in Equation (1). The higher instantaneous turbine power is obtained at the zero-volume due to a higher level of pressure at the turbine inlet. The peak of turbine power with non-volume is 4 times higher than that of the large manifold. This leads to higher mean turbine power over the cycle. The higher turbine power contributes to increasing compressor power. As a result, a higher boost is generated which increases intake air mass flow into the combustion chamber. This results in increasing engine performance as shown in Figure 5 (c).

$$P_T = \dot{m}\, C_p\, \eta_m\, \eta_{isen}\, T_{in}\, (1 - (\frac{1}{PR})^{\frac{k-1}{k}}) \qquad (1)$$

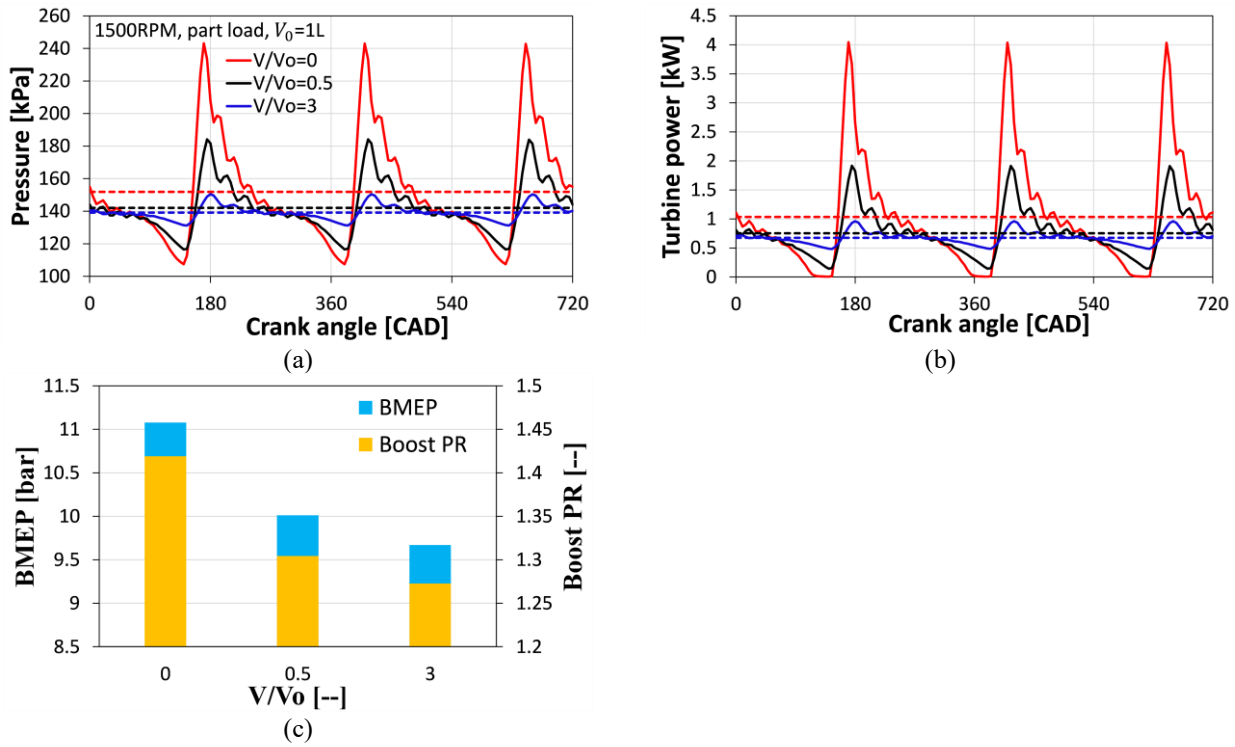

Figure 5. Results of simulation on three different exhaust manifold volumes: (a) Instantaneous exhaust pressure pulse at turbine inlet; (b) Instantaneous turbine power; (c) BMEP and boost PR at 1500 RPM and part load.

From this simulation, it was found that the exhaust manifold volume has a significant impact on the shape of the exhaust pressure pulse at the turbine inlet. A similar finding was observed in the work by Anton et al. (2017), Liu et al. (2021). For the large volume at the turbine upstream, it shows lower peaks of exhaust pressure and low average exhaust pressure. This is mainly associated with the exhaust volume that acts as a pressure damper and resistance. When the exhaust pressure propagates along the pipes and meets up the large manifold, the sudden expansion results in damping of the pressure. In addition, the large volume reduces the exhaust resistance which brings down exhaust backpressure and allows more easy ejection of exhaust gases. For this reason, the lower peak pressure and lower cycle-average pressure are observed at the large volume. Thus, the large volume reduces the exhaust pulsation so that the turbine performance is negatively affected by the low level of pressure energy at the turbine inlet. However, this low exhaust back pressure improves scavenging performance and reduces pumping losses. If a much larger manifold is applied, exhaust pressure and turbine power pulse would be flattened. Then, it will work like constant pressure turbocharging system.

The non-volume in the exhaust manifold demonstrates higher pressure peaks which increase the mean exhaust pressure. The zero volume in the exhaust line imposes high exhaust resistance and no sudden expansion. The high resistance induces high exhaust backpressure since the exhaust can not be pushed out and built up at the exhaust line. This makes the exhaust gases hard to be expelled. This deteriorates the scavenging performance and the pumping losses. However, the high backpressure entails high pulsating exhaust flow which increases the available energy at the turbine inlet. The higher exhaust pressure at the turbine inlet is preferred as the turbine utilizes this pressure energy to generate useful work. Nevertheless, it should be compromised with excessive backpressure and pumping losses. Even though at some points,

instantaneous turbine power is decreased by diminished pressure, however, its decrement is less than the increment. Thus, the loss of instantaneous turbine power is offset, and the overall mean power is increased.

3.2 Length of Exhaust Runner

The effect of length of the exhaust runner was examined based on the engine model with zero exhaust manifold volume (V/V0 = 0) and constant diameter of exhaust runner (D0 = 31 mm). Three different lengths were considered (L/L0 = 0.33, 1 and 2.7, L0 = 76 mm). The results are presented over the cycle in Figure 6. As seen in Figure 6 (a), the shorter runner shows 1.7 times higher peak in exhaust pressure at the turbine inlet than the longer runner. This leads to 3.6 times higher peak in instantaneous turbine power. Thus, the higher mean turbine power is achieved at the shorter runner as shown in Figure 6 (b). The higher turbine power delivers more energy to the compressor. Hence, the higher boost pressure and engine performance (BMEP) are obtained as Figure 6 (c).

The main reason why the short exhaust runner has better pressure energy and performance is related to the volume. The exhaust runner also could be part of the volume. Hence, the short exhaust runner has less volume which increases the exhaust resistance and pumping losses. The increased exhaust resistance by the reduced volume is favorable to preserve the high pulsating pressure. On the other hand, the longer exhaust runner would have larger volume. This improves scavenging performance and lowers exhaust backpressure. Hence, the large volume damps out the exhaust pulsation and turbine power.

However, it is nearly impossible to have zero length at exhaust runners since it is necessary to connect exhaust ports to turbocharger turbine. This does not mean keeping the runner length as short as possible. There is another factor to consider in determining the runner length which is reflected pressure wave. When the exhaust valves open, the pressure wave is generated and then propagated into the exhaust manifold. When the pressure wave encounters any geometrical changes such as sudden expansion, sharp bend, junction, and pipe end, the wave is reflected and propagated back to the valves. If this reflected wave arrives before the end of the exhaust process, it would benefit the scavenging process. Generally, its arrival timing is related with the exhaust geometry such as runner length, diameter, and manifold volume (Kim, 2019). To get the full benefit of a better gas exchange process, it would be considered in the development stage.

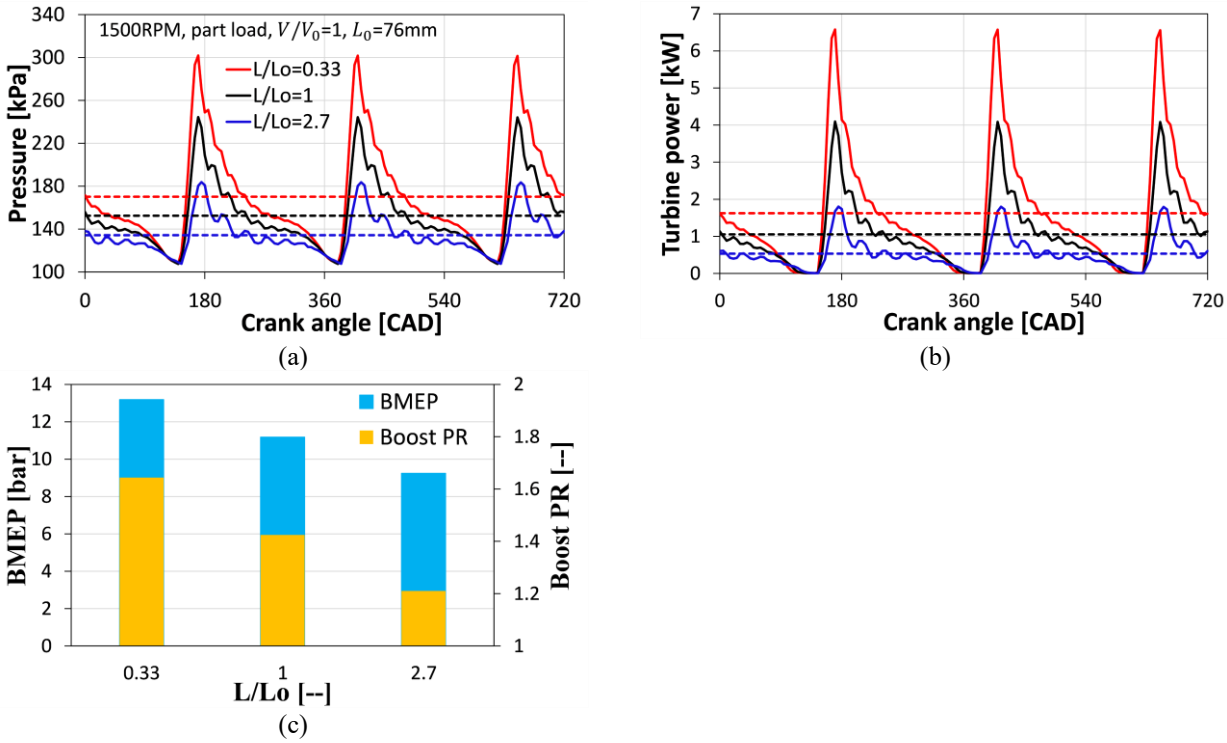

Figure 6. Results of simulation on three different lengths of exhaust runner: (a) Instantaneous pressure pulse at turbine inlet; (b) Turbine power; (c) BMEP and boost PR at 1500 RPM and part load.

The shape of the instantaneous pressure pulse and turbine power is extended upward with decreasing the length of the exhaust runner. However, the lowest pulse peaks are not changed and maintained regardless of runner length compared

to the shapes seen in the manifold volume. Hence, the higher peak affects exhaust pressure and turbine power significantly. After the highest peak pressure, there are several spikes visible while pressure is decreasing.

These small spikes are from the reflected pressure wave. As the length of the runner is shorter, the number of small spikes after the peak pressure is increased. It is because the pressure pulse could travel and be reflected more times in the short runner under the given time. In addition, the spikes are getting weak. The first spike is noticeable but the last one is almost invisible. The reason is that the strength of the pulse is attenuated by traveling & reflecting multiple times and its impact is only significant up to the third pulse order (Sammut and Alkidas, 2007).

3.3. Diameter of Exhaust Runner

The influence of the diameter of the exhaust runner was studied using the engine model with zero exhaust manifold volume (V/V0 = 0). Four different diameters were considered (D/D0 = 0.48, 0.74, 1 and 1.67, D0 = 31 mm). The length of the exhaust runner was maintained (L/L0 = 1). The simulation results are illustrated in Figure 7. The shape of the pressure pulse in Figure 7 (a) has a similar trend as observed in Figure 6 (a). With decreasing the diameter of the runner from D/D0 = 1.67 to D/D0 = 0.74, 1.3 times higher pulsating pressure and 1.9 times higher turbine power are achieved, as shown in Figures 7 (a) and (b). The boost pressure and BMEP are improved since larger turbine work is generated and transferred to the compressor as seen in Figure 7 (c). It is mainly attributed to the exhaust volume as explained before. The smaller diameter reduces the runner volume and increases the exhaust resistance. Even though it increases exhaust backpressure, it improves the utilization of pulsating pressure energy. Also, the reduced runner diameter accelerates exhaust velocity which contributes to increasing exhaust enthalpy. The turbine could recover more energy from the exhaust.

It was perceived that the lesser volume by the decreased diameter to some extent did increase the pulsating pressure and engine performance as similar to the manifold volume and length of the exhaust runner. However, the excessively reduced diameter (D/D0 = 0.48) shows decreased peak pressure pulse, turbine power, boost PR and BMEP in sequence. In fact, too narrow runner diameter increases friction and pressure drop further (Watson and Janota, 1982). Hence, most of the pulsating pressure energy is utilized to compensate for the increased losses and then less energy is left and transferred to the turbine so that the lower boost pressure and BMEP are obtained. Therefore, too narrow runner diameter should be avoided to prevent the performance degradation of the engine and the turbocharger.

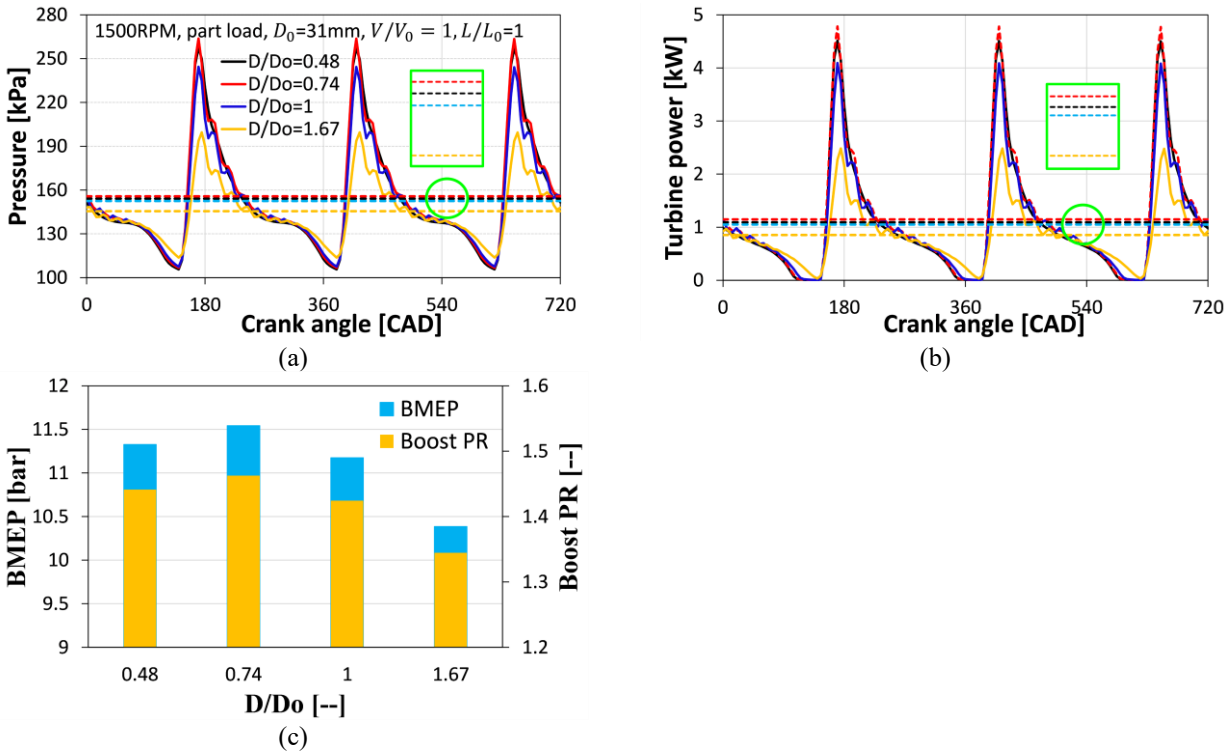

Figure 7. Results of simulation on four different diameters of exhaust runner: (a) Instantaneous pressure pulse at turbine inlet; (b) Turbine power; (c) BMEP and boost PR at 1500 RPM and part load.

In the aspect of engine operation, the narrow pipe diameter is not recommended as it constrains maximum flow rate and causes high back-pressure which results in poor scavenging and high pumping loss. The compromise between exhaust back-pressure, flow rate, and pulse utilization should be considered to determine the correct diameter of the exhaust runner. From the simulation results, the minimum diameter shall be between 0.48 and 0.74 of D/D0 at the current operating point.

In regard to the pulse shape influence on the exhaust pressure and turbine power, it shows a similar trend to that of the exhaust runner length. The lower peak is maintained, and only the high peak shows some difference with varying diameter of the exhaust runner. However, If D/D0 is below 1, its increments are not that significant. For this reason, the mean pressure and turbine power are overlapped in one single line.

3.4. Further Investigation on the Effect of Exhaust Manifold Volume

From extensive parametric study, it was identified that the turbine upstream geometry has a great effect on pulsating exhaust flow, exhaust energy, and turbocharger & engine performance to some extent. In particular, the volume before the turbine is strongly correlated with exhaust resistance, exhaust flow pulsation, and exhaust energy. Therefore, its impact is investigated further under full load.

Two different models were set up: one is with an exhaust manifold (V/V0 = 1), and another is without exhaust manifold volume (V/V0 = 0). The steady-state simulation was extended over different engine speeds from 1000 to 4000 RPM with an increase of 500 RPM. In these additional simulations, WG is controlled to match the given maximum target torque instead of a fully closed position which is plotted in Figure 8 (a). If excessive torque is detected, the WG opens additionally. Otherwise, the WG is closed. The simulation results are presented in Figure 8.

The target torque is achieved from 1500 to 4000 RPM for both cases but is not achieved at low speed (1000 RPM) as shown in Figure 8 (a). It is mainly attributed to low exhaust enthalpy at low-speed regions. Basically, the mass flow rate is far lower at low engine speed which is not sufficient to spool up the turbine. As a result, the compressor is not able to deliver the required boost pressure to achieve the target torque.

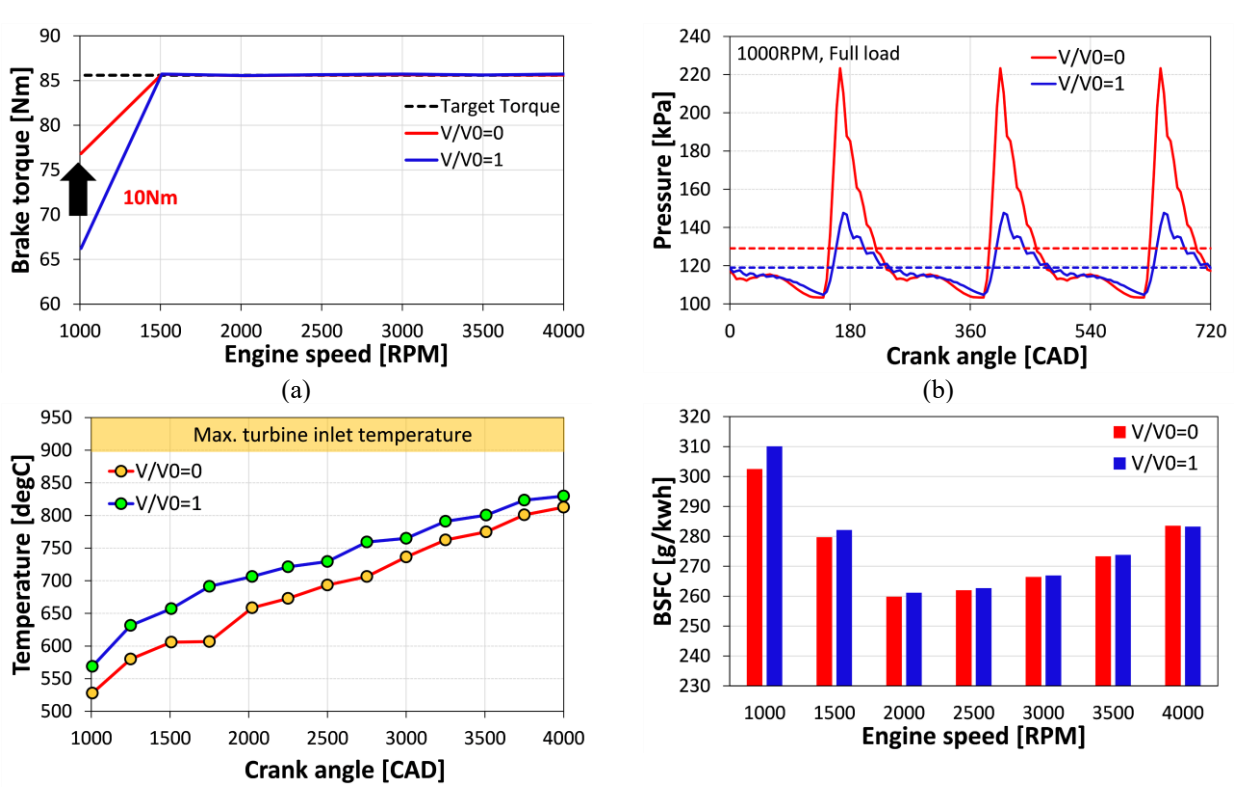

Figure 8. Steady-state simulation results over different engine speeds: (a) Brake torque; (b) Instantaneous turbine inlet pressure; (c) Exhaust temperature; (d) BSFC.

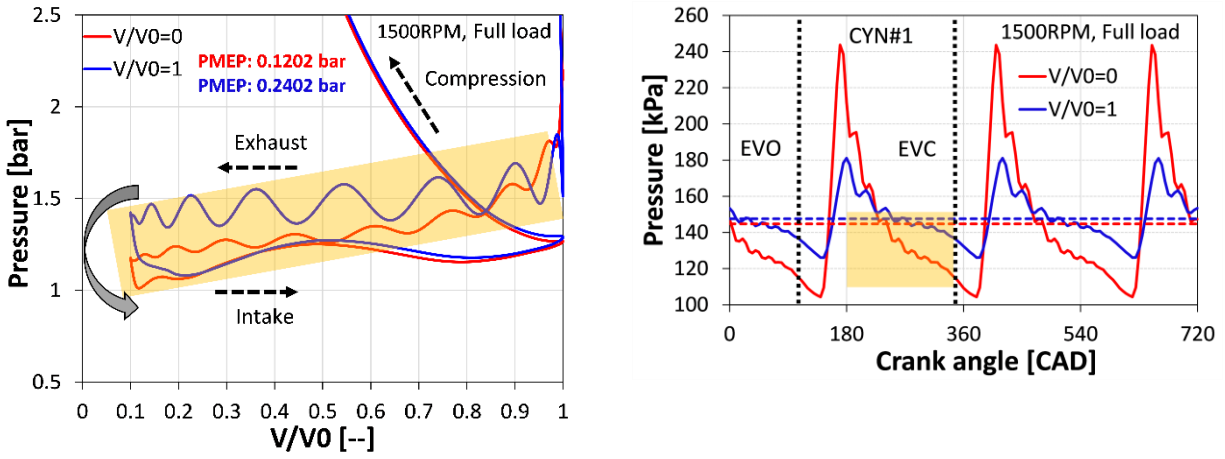

(a) (b)

Figure 9. (a) P-V diagram of cylinder No.1 and (b) Instantaneous turbine inlet pressure (or exhaust backpressure) at 1500 RPM and full load.

Even though the target torque is not achieved at 1000 RPM, the non-exhaust volume model (V/V0 = 0) shows higher torque improvement by 10 Nm (15 %) against the volume model (V/V0 = 1). It is because of the highly pulsating pressure. As shown in Figure 8 (b), 1.5 times higher pulsating pressure is obtained at zero exhaust manifold volume. The increased exhaust resistance by the reduced volume hinders exhaust flow which contributes to increasing pressure peaks during the blow-down phase. Thus, the higher turbine power is obtained by increased energy at the turbine inlet so that the compressor is able to deliver higher boost pressure which results in higher brake torque. From this, it is noted that the smaller exhaust manifold volume could improve low-speed torque.

While carrying out the full load simulation, exhaust temperature was monitored which is illustrated in Figure 8 (c). The exhaust temperature of the gasoline engine is hotter than the diesel counterpart. For this reason, the exhaust temperature should be carefully monitored in the gasoline engines. In general, the maximum threshold of the turbine inlet temperature is between 900 °C and 950 °C due to the durability of the turbine. In general, if the exhaust temperature is high, more fuel is injected to bring down combustion and exhaust temperature at the cost of BSFC penalty.

The exhaust temperature of the volume model (V/V0 = 1) indicates slightly higher temperature compared to the non-volume model (V/V0 = 0). It is mainly associated with pumping loss. As presented in Figure 10 (a), higher PMEP is observed at the volume model. Thus, to achieve the same target torque, more air and fuel are needed to offset the pumping loss. As a result, the exhaust temperature is increased by invigorating combustion. It will be discussed why higher PMEP is achieved in the volume model in the later part.

In fact, the turbine inlet temperature (or exhaust temperature) contributes to turbine power as seen in Equation (1). However, in our case, the temperature difference is not that significant. Its contribution is not that much. Instead, the pulsating pressure pulse (in the form of PR) is a major factor to determine the turbine power which is clearly observed in Figure 8 (b) and Figure 9 (b).

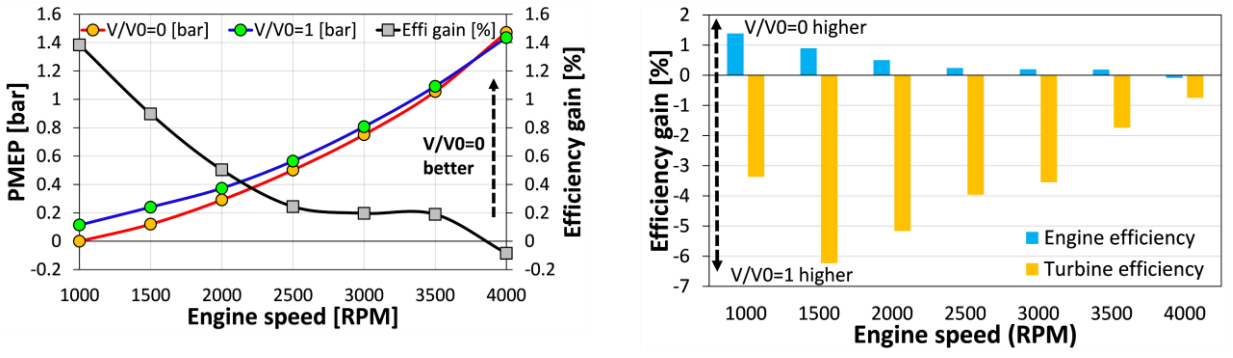

(a) (b)

Figure 10. (a) PMEP and engine efficiency gain over different engine speeds at full load and (b) Engine and turbine efficiency gain.

BSFC is plotted in Figure 8 (c) and non-manifold volume shows better BSFC over wide speed regions. With increasing engine speeds, its BSFC gain is steadily reduced. Especially, at 4000 RPM, the BSFC is slightly degraded for the non-volume model. The observed results are somewhat different from what we know. In general, the non-volume or smaller volume in the exhaust line or turbine upstream is expected to increase the BSFC due to high exhaust resistance and backpressure. In most cases, this is well accepted. However, in the current study, the conflicting results are observed. Hence, the further analysis has been conducted based on cyclic data and P-V diagram is utilized as shown in Figure 9 (a).

The enclosed area between exhaust and intake process in the P-V diagram represents the pumping work. Since the area of the non-volume model (V/V0 = 0) is smaller than that of the volume model (V/V0 = 1), less pumping work is carried out by the engine. In order to quantify the pumping losses, pumping mean effective pressure (PEMP) was introduced which describes the pumping work per given displacement volume as presented in Equation (2).

$$\text{PMEP [bar]} = \frac{\int (p_{exhaust} - p_{boost}) dv}{V_d} \qquad (2)$$

Compared to the volume model, the non-volume model significantly reduced the pumping losses by half. In order to achieve same torque or BMEP (1500 ~ 4000 RPM), the less work is required by the engine due to the reduced pumping losses. Hence, less fuel is consumed which improves BSFC in the case of the non-volume model. The reduced pumping loss is resulted from the decreased in-cylinder pressure during the exhaust phase. This low in-cylinder pressure is mainly attributed to large exhaust pulsation, as highlighted by yellow in Figure 9 (b). This large pulsation is generated by high exhaust resistance from the reduced exhaust volume.

Basically, the exhaust process can be divided into two phases. One is a blow-down phase (EVO to BDC) where a large portion of exhaust gases is expelled. Another is an exhaust phase (BDC to EVC) after blow-down process where the piston is moving upward (TDC) to push out the remaining exhaust gases. The high back-pressure during the blow-down phase is not a matter as the in-cylinder pressure is far much higher by combustion. Hence, the large and positive pressure gradient between the cylinder and exhaust line could overcome the high back-pressure and discharge the exhaust gases. The positive work is done by the engine until TDC.

However, the high backpressure during the exhaust phase after TDC could hamper the scavenging process due to less pressure gradient since in-cylinder pressure fall close to ambient. To overcome the high backpressure, a higher in-cylinder pressure is required which results in high pumping loss and deteriorates fuel consumption. On the other hands, the lower exhaust back-pressure by the non-volume during gas exchange period, facilitates scavenging process. Hence, in the next cycle, the more air would be drawn and volumetric efficiency can be improved which reduces boosting demand. Therefore, the lower exhaust pressure is favorable condition, especially during the exhaust phase.

This condition was achieved by removing the volume of the exhaust manifold as it eliminates pressure damping in the exhaust line. As shown in Figure 9 (b), the lower exhaust pressure of the non-volume model after BDC contributes to decreasing the pumping work and then improving the fuel consumption. Even though there is a higher pressure at the early part of the exhaust phase (right after BDC), this can be offset as it is a relatively short period. Therefore, it does not have a significant effect on the pumping loss.

The higher backpressure increases the residual fraction due to poor scavenging performance. The increased residual fraction could lead to engine knocking which is critical in the gasoline engines, especially under full load operations. Mostly, the full load and low-speed regions are vulnerable to the knocking due to high boost because the low-speed regions generally have low volumetric efficiency against high speed regions. In our study, the non-volume model showed lower exhaust backpressure which suppresses the knocking intensity and improves knocking margin at the full load operation. In addition, this low backpressure (the non-volume model) could help to improve low-speed torque further without engine knocking. On top of that, the reduced knocking intensity could help to reduce fuel consumption. Under the full load operation, the reduced knocking allows to maintain MBT timing. However, in case of the high knocking propensity, the ignition timing should be retarded which increase fuel consumption. For this reason, the non-volume model has better potential to improve low-speed torque and fuel consumption under the full load operation.

The PMEP and engine efficiency gain are plotted over different engine speeds in Figure 10 (a). It is noted that the differences of PEMP between the volume and non-volume model are directly proportional to the efficiency gain. The positive efficiency gain indicates how many percent of the engine efficiency is improved by the non-volume model against the volume model. It is calculated as Equation (3).

$$Efficiency\ gain\ [\%] = \frac{(\eta_{V/V0=0} - \eta_{V/V0=1})}{\eta_{V/V0=1}} \times 100 \qquad (3)$$

The larger the difference of the PMEP is, the higher the efficiency gain is. It represents that the higher reduction of PMEP results in enhancing the engine efficiency and fuel consumption which are achieved by zero-exhaust volume. The higher efficiency gain is obtained at 1000 RPM by 1.4%, while the efficiency gain is slightly degraded by 0.08% at 4000 RPM due to increased PMEP.

Engine and turbine efficiency gain are plotted in Figure 10 (b). The turbine efficiency gain is calculated in the same manner as the engine efficiency gain. For both parameters, the positive number indicates better efficiency by zero exhaust volume model, while the negative number represents better efficiency by the volume model. It is seen that engine and turbine efficiency gain show different trend. The non-exhaust volume model indicates slight improvement in the engine efficiency but a large drop in turbine efficiency. On the other hand, the volume model presents better efficiency in the turbine but not in the engine. In order to understand this odd trend, instantaneous turbine mass flow (in terms of mass flow parameter) and turbine efficiency are examined at 2000 RPM which are presented in Figure 11. The following parameters are calculated by equation (4) and equation (5).

$$MFP\ [kg.\sqrt{K}/\ s.bar] = \frac{\dot{m}\sqrt{T_{in}}}{P_{in}} \tag{4}$$

$$\eta_T = \frac{h_{in} - h_{out}}{T_{in} C_p \times \left[1 - \left(\frac{P_{out}}{P_{in}}\right)^{\frac{k-1}{k}}\right]} \tag{5}$$

The decreased turbine efficiency in the non-manifold volume model is related with the exhaust volume. The non-volume in the exhaust manifold contributed to dropping mass flow at the turbine inlet as shown in Figure 11 (a). However, the volume in the exhaust manifold did not allow a sharp decrease of the mass flow in the turbine entry as the large volume prevents variation or fluctuation to some extent by working as a flow damper. Also, the exhaust gases are piled up at the manifold volume and the pre-occupied gases from other cylinders or previous cycles will interrupt sharp mass flow drop. As a result, the sharp drop in instantaneous mass flow leads to decreasing turbine efficiency as illustrated in Figure 11 (b).

The sharp drop in flow and pressure would bring down turbocharger speed. To get back to the initial level of pressure, the turbocharger should be accelerated. In this deacceleration and acceleration process, more energy would be wasted by the turbine in case of the non-volume model due to a large drop. Thus, the turbine efficiency is degraded. Theoretically, the large variation of mass flow develops unsteady flow conditions which make incidence angle far from the designed value. This results in large incidence loss and low turbine efficiency. However, this is three-dimensional phenomenon. 1D engine simulation is not able to capture this, as the turbocharger performance is predicted by compressor and turbine map. Thus, the turbine efficiency would not be discussed in detail in this study.

In short, the zero-volume in the exhaust manifold improves fuel economy and engine efficiency which are dependent on exhaust backpressure and PMEP. The high exhaust pressure pulsation at turbine inlet during exhaust phase in the non-volume induced low PMEP. However, the sharp drop in instantaneous mass flow at the turbine inlet decreased the turbine efficiency. Nevertheless, the non-volume has the potential to improve low-speed torque, fuel consumption, scavenging, and knocking.

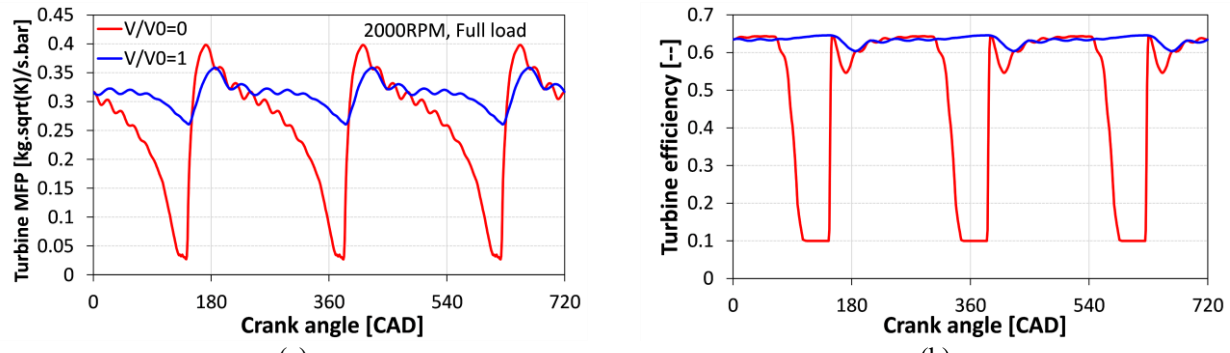

(a) (b)

Figure 11. (a) Turbine MFP and (b) Turbine efficiency at 2000 RPM and full load.

4. CONCLUSIONS

The decreased turbine efficiency in the non-manifold volume model is related with the exhaust volume. The non-volume in the exhaust manifold contributed to dropping mass flow at the turbine inlet as shown in Figure 11 (a). However, the volume in the exhaust manifold did not allow a sharp decrease of the mass flow in the turbine entry as the large volume prevents variation or fluctuation to some extent by working as a flow damper. Also, the exhaust gases are piled up at the manifold volume and the pre-occupied gases from other cylinders or previous cycles will interrupt sharp mass flow drop. As a result, the sharp drop in instantaneous mass flow leads to decreasing turbine efficiency as illustrated in Figure 11 (b).

The ramification of the turbine upstream geometry: exhaust runner length, runner diameter, and manifold volume on the pulsating flow and performance of engine & turbocharger has been investigated using 1D engine simulation. A validated SI engine model was utilized as a base engine. Firstly, the parametric study was carried out to examine its influence at a single operating point. Then, an additional investigation was conducted under full load to deeply comprehend how exhaust manifold volume interacts with the pulsating flow and engine & turbocharger behavior. The key findings are summarized as follows:

(1) Turbine upstream geometry has influenced the shape of pulsating pressure profile, exhaust energy and engine performance. Even though the pulsating flow is dependent on engine operating conditions, its utilization can be enhanced further at certain turbine upstream geometry configuration.

(2) The significant geometry factor is the volume in the exhaust line before the turbine. The reduced volume (short runner length, smaller runner diameter, and smaller manifold volume) induced higher pulsating flow which contributes to increasing exhaust energy to be recovered by the turbine. This increased boost pressure and engine performance.

(3) The non-exhaust manifold (V/V0 = 0) showed better low-speed performance due to increased pressure amplitude (high-pressure pulsation) and exhaust energy over the original manifold (V/V0 = 1). At 1000 RPM, 10 Nm (15 %) higher brake torque was obtained against the existing volume model (V/V0 = 1). Besides, 2.4 % lower BSFC was achieved.

(4) Under the same brake torque conditions (1500 ~ 4000 RPM), the zero-exhaust volume model demonstrated lower backpressure and pumping losses compared to the volume model. As a result, the brake thermal efficiency and BSFC were improved up to 0.9 % and 0.8 %, respectively. However, the turbine efficiency was negatively affected by 6 % due to a sharp drop in mass flow.

(5) The non-volume in the exhaust manifold has more potential to suppress the knocking due to the low residual fraction from the reduced exhaust backpressure. This has the potential to enhance BSFC, especially at the full load operation.

(6) It is beneficial to minimize unnecessary volume in the exhaust line in exploiting unsteady pulsating flow energy by the turbocharger turbine. The effective utilization of pulsating energy gives rise to improving pumping losses, scavenging performance, engine knocking, engine performance, thermal efficiency, and fuel economy moderately.

ACKNOWLEDGEMENT– The author would like to thank AVL GmbH for providing an academic license to carry out this research.

REFERENCES

Al-Hasan, N., Beer, J., Ehrhard, J., Lorenz, T. and Stump, L. (2015). Charging technologies for CO2 optimization by millerization. SAE Paper No. 2015-01-1250.

Alshammari, M., Alshammari, F. and Pesyridis A. (2019). Electric boosting and energy recovery systems for engine downsizing. Energies 12, 24, 4636.

Anton, N., Genrup, M., Fredriksson, C., Larsson, P. I. and Erlandsson-Christiansen, A. (2017). Exhaust volume dependency of turbocharger turbine design for a heavy duty otto cycle engine. ASME Turbo Expo: Power for Land, Sea, and Air, Charlotte, North Carolina, USA.

AVL (2014). BOOST Ver. 2014.1 User Guide.

Bassett, M., Hall, J., Cains, T., Underwood, M., Wall, R. and Richard, B. (2017). Dynamic downsizing gasoline demonstrator. SAE Int. J. Engines 10, 3, 884–891.

Brace, R. (2020). https://www.realclearenergy.org/articles /2020/11/29/five_reasons_why_internal_combustion_engines_are_here_to_stay_651051.html

Cao, K., Yang, M. and Martinez-Botas, R. (2015). A numerical investigation on a new pulse-optimized flow control method for turbocharger turbine performance improvement under pulsating conditions. ASME Turbo Expo: Power for Land, Sea, and Air, Montreal, Quebec, Canada.

Chiong, M., Abas, M., Tan, F., Rajoo, S., Martinez-Botas, R., Fujita, Y., Yokoyama, T., Ibaraki, S. and Ebisu, M. (2019). Steady-state, transient and WLTC drive-cycle experimental performance comparisons between single-scroll and twin-scroll turbocharger turbine. SAE Paper No. 2019-01-0327.

Christmann, R., Weiskes, S., Rohi, A. and Gugau M. (2020). BorgWarner turbochargers with variable turbine geometry (VTG). https://www.autotecnica.org/borg warner-turbochargers-with-variable-turbine-geometry/

Feneley, A., Pesiridis, A. and Andwari, A. (2017). Variable geometry turbochargers technologies for exhaust energy recovery and boosting–A review. Renewable and Sustainable Energy Reviews, 71, 959–975.

Ferguson, C. R. and Kirkpatrick, A. T. (2001). Internal Combustion Engines: Applied Thermosciences. 2nd edn. John Wiley & Sons. New York, NY, USA.

Kesgin, U. (2005). Study on the design of inlet and exhaust system of a stationary internal combustion engine. Energy Conversion and Management 46, 13-14, 2258– 2287.

Kim, J. (2019). A Pulse Turbocharging System for Small SI-Engine to Improve Low-End Torque. M. S. Thesis. Universiti Teknologi Malaysia. Johor, Malaysia.

Kusztelan A., Marchant, D., Yao, Y., Wang, Y., Selcuk, S. and Gaikwad, A. (2012). Increase in low speed response of an IC engine using twin-entry turbocharger. Proc. World Cong. Engineering (WCE), London, UK.

Lim, S., Dahljild A. and Mihaescu, M. (2018). Influence of upstream geometry on pulsatile turbocharger turbine performance. ASME Turbo Expo: Power for Land, Sea, and Air, Oslo, Norway.

Liu, F., Sun., C., Li. Y. and Shang, Y. (2021). Performance analaysis and optimization design of exhaust system for turbocharging diesel engines. Int. J. Automotive Technology 22, 3, 735–745.

Lou, Z. and Zhu, G. (2020). Review of advancement in variable valve actuation of internal combustion engines. Applied Sciences 10, 4, 1–10.

Mahabadipour, H., Krishnan, S. R., and Srinivasan, K. K. (2018). Investigation of exhaust flow and exergy fluctuations in a diesel engine. Applied Thermal Engineering, 147, 856–865. More, A. (2020). https://www.wfmj.com/story/42642646/ global-turbo-charger-market-2020-top-countries-data-sha re-scope-stake-trends-industry-size-sales-amp-revenue-gr owth-opportunities-and-demand-with

Pesiridis, A. (2012). The application of active control for turbocharger turbines. Int J. Engine Research 13, 4, 385– 398.

Rajoo, S., Pesiridis, A. and Martinez-Botas, R. (2013). Novel method to improve engine exhaust energy extraction with active control turbocharger. Int J. Engine Research 15, 2, 236–249.

Reitz, R., Ogawa, H., Payri, R., Fansler, T., Kokjohn, S., Moriyoshi, Y., Agarwal, A., Arcoumanis, D., Assanis, D., Bae, C., Boulouchos, K., Canakci, M., Curran, S., Denbratt, I., Gavaises, M., Guenthner, M., Hasse, C., Huang, Z., Ishiyama, T., Johansson, B., Johnson, T., Kalghatgi, G., Koike, M., Kong, S., Leipetz, A., Miles, P., Novella, R., Onorati, A., Richter, M., Shuai, S., Siebers, D., Si, W., Trujillo, M., Uchida, N., Vagileco, B., Wanger, R. and Zhao, H. (2019). IJER editorial: the future of the internal combustion engine. Int. J. Engine Research 21, 1, 3–10.

Sammut, G. and Alkidas, A. (2007). Relative contributions of intake and exhaust tuning on SI engine breathing – A computational study. SAE Paper No. 2007-01-0192.

Shahed, S. (2006). An analysis of assisted turbocharging with light hybrid powertrain. SAE Paper No. 2006-01-0019.

Terdich, N., Martinez-Botas, R., Romagnoli, A. and Pesiridis, A. (2014). Mild hybridization via electricfication of the air system: electrically assised and variable geometry turbocharging impact on an off-road diesel engine. J. Engineering for Gas Turbines and Power 136, 3, 1–12.

Turner, J., Popplewell, A., Patel, R., Johnson, T., Darton, N., Richardson, S., Bredda, S., Tudor, R., Bithell, C., Jackson, R., Remmert, S., Cracknell, R., Fernandes, J., Lewis, A., Akehurst, S., Brace, C., Copeland, C., Martinez-Botas, R., Romagnoli, A. and Burluka, A. (2014). Ultra boost for economy: extending the limits of extreme engine downsizing. SAE Int. J. Engines 7, 1, 387–417.

US EPA (2020). The 2019 EPA automotive trends report. Executive Summary. EPA-420-S-20-001.

Watson, N. and Janota, M. S. (1982). Turbocharging the Internal Combustion Engine. 1st edn. Palgrave Macmillan. London, UK.

Xue, X. and Rutledge, J. (2017). Potentials of electrical assist and variable geometry turbocharging system for heavy-duty diesel engine downsizing. SAE Paper No. 2017-01-1035.